Prepinted version
Published version DOI: /10.1016/j.snb.2020.128948
Sensors & Actuators B: Chemical 327 (2021) 128948

Wireless wearable wristband for continuous sweat pH monitoring

Pablo Escobedo,[e] Celia E. Ramos-Lorente,[a] Antonio Martínez-Olmos,[b,d] Miguel A. Carvajal,[b,d] Mariano Ortega-Muñoz,[c,d] Ignacio de Orbe-Payá,[a,d] Fernando Hernández-Mateo,[c,d] Francisco Santoyo-González,[c,d] Luis F. Capitán-Vallvey,[a,d] Alberto J. Palma,[b,d] Miguel M. Erenas[a,d]

[a] *ECsens, Department of Analytical Chemistry, Faculty of Sciences, Campus Fuentenueva s/n, University of Granada, 18071-Granada, Spain*
[b] *ECsens, Department of Electronics and Computer Technology, ETSIIT C/Pta. Daniel Saucedo Aranda s/n, University of Granada, 18071-Granada, Spain.*
[c] *Department of Organic Chemistry, Biotechnology Institute, Faculty of Sciences, Campus Fuentenueva s/n, University of Granada, 18071-Granada, Spain*
[d] *Unit of Excellence in Chemistry applied to Biomedicine and the Environment of the University of Granada.*
[e] *Bendable Electronics and Sensing Technologies (BEST) Group, University of Glasgow, Glasgow, G12 8QQ, UK*

Abstract

Several studies have shown that the determination of pH in sweat, which is one of the most accessible body fluids, can be an indicator of health and wellness, and even be used for potential disease diagnosis. On that basis, we present herein a wearable wristband for continuous and wireless monitoring of sweat pH with potential applications in the field of personal health assessment. The developed wristband consists of two main parts: a microfluidic cloth analytical device (μCAD) to collect continuously the sweat from skin with a colour-based pH sensing area; and a readout and processing module with a digital color sensor to obtain the pH of sweat from the color changes in the μCAD. In addition, the readout module includes a low-power Bluetooth interface to transmit the measurements in real-time to a custom-designed smartphone application. To allow continuous operation, an absorbent pad was included in the design to retire and store the sweat from the sensing area through a passive pump path. It was found that the Hue parameter (H) in the HSV color space can be related to the sweat pH and fitted to a Boltzmann equation (R^2=0.997). The range of use of the wristband device goes from 6 to 8, which includes the pH range of sweat, with a precision at different pH values from 3.6 to 6.0 %. Considering the typical human sweat rate, the absorbent pad allows continuous operation up to more than 1000 minutes.

Keywords: pH sensor; Sweat analysis; Microfluidic cloth analytical device (μCAD); Wearable system; Wireless monitoring; Smartphone.

1. Introduction

Wearable technology has significantly evolved in the last years with the advent of products such as smartwatches and wristbands. In particular, the use of wearables for personal health assessment has fuelled the growth of these devices by enabling non-invasive methods for continuous monitoring of physical activity and vital signs (An et al., 2017; Jeong et al., 2019). Not surprisingly, the wearable fitness technology market was valued at $5.77 billion in 2016 and it is expected to be worth $12.44 billion by 2022, growing at an estimated compound annual growth rate (CAGR) of 13.7% from 2016 to 2022 (MarketsandMarkets, 2016). Among the different physiological parameters of interest, we must highlight the monitoring of heart rate (Chacon et al., 2018), blood pressure (Boutry et al., 2019; Riaz et al., 2019), respiration rate (Güder et al., 2016), body temperature (Manas et al., 2018) and sweat (Gao et al., 2016; Liu et al., 2016; Martín et al., 2017; Nyein et al., 2018). In contrast with traditional health monitoring instruments, wearable devices have some key advantages such as portability, ubiquity or ease of use, and they are able to provide continuous, real-time, wireless monitoring of health conditions in a non-invasive way (Gao et al., 2019; Ortega et al., 2019; Parrilla et al., 2019; Xu et al., 2019).

Several studies have shown that analytes of interest in blood such as glucose, lactate, urea or sodium, to name but a few, are also found in other biofluids sources such as saliva, tears or sweat (Heikenfeld et al., 2019). The main advantage of using these alternative biofluids lies in their easier access, thus avoiding the need for acquiring blood samples and allowing peripheral biochemical monitoring (Chung et al., 2019; Zhao et al., 2020). Sweat is particularly attractive since it is one of the most accessible body fluids, and it can even be produced by on-demand stimulation using techniques such as iontophoresis (Kim et al., 2018). pH determination in sweat is an indicator of health and wellness, and it can be used even for potential disease diagnosis. Under normal conditions, the pH of healthy human sweat is within the range from 4.5 to 7.0. Nevertheless, the pH of our sweat can vary dramatically under circumstances of homeostasis dysregulation, disease, acidosis and even stress (Perry, 2018). For instance, cystic fibrosis patients are reported to have a higher pH (up to pH 9) than normal individuals (Nikolajek and Emrich, 1976), and sweat pH can be also used as an indicator of metabolic alkalosis (Patterson et al., 2002). In the field of sport and exercise, it is well known that the formation and evaporation of sweat is the principal means of heat removal. If the sweat losses lead to a body water deficit or hypohydration, the reduced volume of body fluids will contain a greater concentration of sodium (Na^+) and potassium (K^+), which can cause hypertonic hypovolemia (Sawka and Coyle, 1999). Severe dehydration can lead to headache, vomiting, muscle cramping, dizziness, nausea and even fainting. In this context, sweat pH can be used to monitor exercise intensity and dehydration since it is associated with sodium concentration (Curto et al., 2012). On the other hand, excessive water intake can cause hyponatremia, which refers to a low sodium concentration. Clinical features of symptomatic hyponatremia include seizures, pulmonary edema, muscle fasciculation, disorientation, mental confusion, respiratory arrest, weakness, nausea and even coma

(Noakes, 1992). Therefore, the reliable monitoring of sweat pH is crucial for health assessment and wellness monitoring applications (Kaya et al., 2019).

Different approaches for wearable sweat pH monitoring can be found in the literature over the last few years. According to their sensing strategy, a number of platforms draw upon optical colorimetric detection (Bandodkar et al., 2019; He et al., 2019; Ahyeon Koh et al., 2016; Lopez-Ruiz et al., 2014; Morris et al., 2009; Nyein et al., 2018), while others make use of electrochemical pH sensors (Anastasova et al., 2016; Bandodkar et al., 2019; Dang et al., 2018) reviewed by Chung et al. (Chung et al., 2019). In the first case, the use of microfluidic devices allows the precise positioning of the reagents in a specific test zone to which the sweat is guided, thus taking place the desired reaction with the subsequent color change (Choi et al., 2018).

The study of the evolution on time of sweat both rate and composition in different areas of the body has been approached in two main ways referred to passive sampling: *i)* microchannel-based microfluidics that rely on deterministic capillary, the so-called capillary microfluidic (Olanrewaju et al., 2018). In this case, epidermal microfluidic systems that combine channels, valves, mixers, and reservoirs, are able to capture, route, and store microliters of sweat in a time-controlled manner (Choi et al., 2018); or *ii)* porous capillary microfluidics that rely on stochastic capillary flow within a network of pores (paper, cloth, thread) in which the sweat is collected, and delivered to the sensing area being removed by an adsorbent acting as a passive pump (Curto et al., 2012).

To make the system truly wearable and portable, a wireless interface is required to transmit the measured data to the end user. Many systems include a radiofrequency identification (RFID) solution, usually a Near Field Communication (NFC) link (Boada et al., 2019; Dang et al., 2018; Ahyeon Koh et al., 2016). This approach allows the development of passive systems by means of energy harvesting from the electromagnetic field of an external reader, typically an NFC-enabled smartphone. Moreover, the NFC antenna required for this design can be manufactured in flexible and conformable substrates, even stretchable (Bandodkar et al., 2019; Dang et al., 2018). However, this approach is not suitable for continuous, real-time sweat monitoring, since it requires that the external reader is permanently placed close to the system. To overcome such limitations, other systems employ longer range wireless technologies such as Wi-Fi (Kansara et al., 2018; Lu et al., 2019) or Bluetooth (Alizadeh et al., 2018; Anastasova et al., 2016; Nyein et al., 2018).

In this work, we present a wearable wristband for sweat pH monitoring. As Fig. 1 shows, the system comprises two main parts: *i)* a custom-designed microfluidic cloth analytical device (μCAD) to collect and store the sweat that includes a color-based pH sensor built by immobilization of a vinyl sulfone acidochromic dye (**AD-VS**) on a cotton cloth; and *ii)* a miniaturized readout module to obtain the pH measurements from the sensor and extra circuitry to interface with the end user. The proposed wristband allows continuous monitoring of sweat pH and real-time wireless transmission of the measurements to a smartphone via Bluetooth.

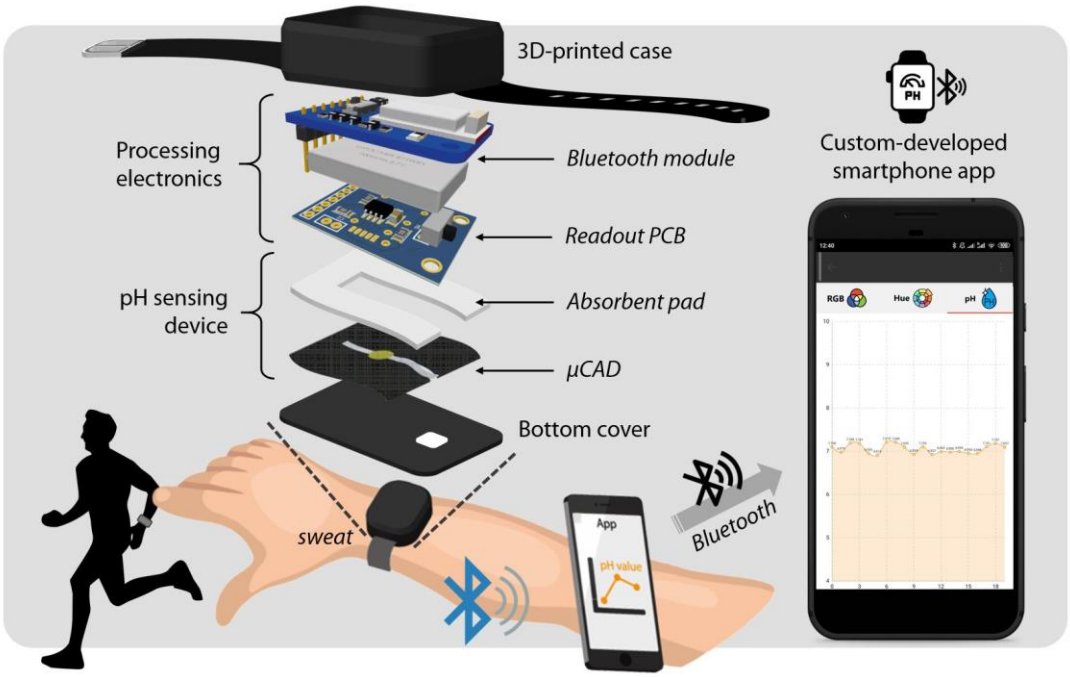

Fig. 1. Exploded view of the wireless wearable wristband, consisting of the custom-designed µCAD with a colorimetric pH sensor and a miniaturized readout module to obtain the pH information from the sensor. Real-time measurements of sweat pH are transmitted to the user smartphone via Bluetooth through a custom-developed app.

2. Materials and Methods

2.1. µCAD design and fabrication

Firstly, a piece of 13.8×17.4 cm^2 of cotton cloth, previously characterized by us in terms of Washburn constant (see Section S8), was screen-printed using a 43 lines·cm^{-1} frame together with a black plastisol ink, to pattern 12 hydrophilic sections as shown in Fig. S8. Lately, the large piece of cotton cloth was cut to obtain each pattern independently, that will be used to prepare the µCAD. Once the cotton patterned cut was obtained, the immobilization of the vinyl sulfone acidochromic dye **AD-VS-1** (Fig. 2(a)) was carried out following the procedure next described. Firstly, it was introduced in a Na_2CO_3 10 mg·mL^{-1} solution for 1 h to scour the screen-printed fabric and improve its capillary properties, as well as to get a basic media on the cloth that makes possible the click immobilization of the **AD-VS-1** via oxa-Michael addition by adding of 0.2 µL of **AD-VS-1** 15 mg·mL^{-1} in DMSO. Afterwards, the cloth was located in a light-safe and let dry for 24 h, and then washed to remove the excess of **AD-VS-1** by sonication in Tris buffer pH=9.2, purified water and methanol, 10 minutes each. Finally, the µCAD was placed in the bottom of the designed holder and, on top of it, the U-shaped absorbent pad as shown in Fig. 2(b-c). The µCAD, as well as the U-shaped absorbent pad, are disposable components that can be replaced when necessary. To collect the sweat, a piece of the sampling path passes through a hole at the bottom cover of the 3D-printed case, being in touch with the skin and collecting the sample while sweating.

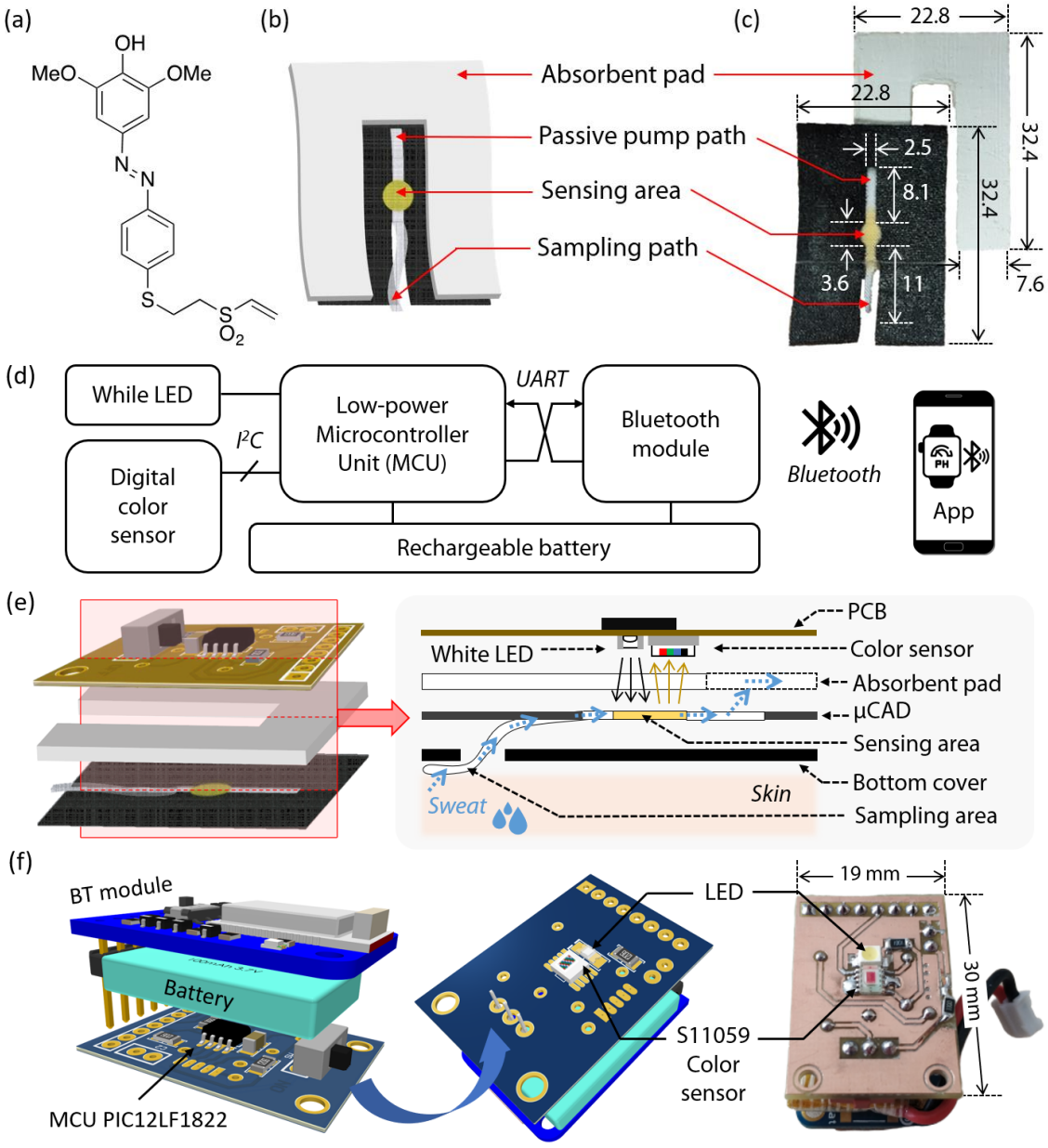

Fig. 2. (a) Chemical structure of **AD-VS-1**; (b) µCAD design; (c) µCAD photograph; (d) Block diagram of the processing electronics in the readout module; (e) Schematic diagram of the sensing procedure in which the LED and color sensor are placed in front of the sensing area of the µCAD; (f) 3D views and real image of the fabricated module with its main components labelled.

In humans, the rate of sweating is around 1250 $g \cdot m^{-2} \cdot h^{-1}$ when exercising (Godek et al., 2008). For that reason, both the sampling and the sensing areas in the µCAD design had to be small enough to avoid the need of high volumes of sample. On the other hand, however, the sensing area needed to have a minimum diameter of 3.6 mm so that the detector included in the device could perform reliable measurements. Cotton cloth was selected as the support for the µCAD because it presents better properties than paper in terms of flexibility and bending resistance. However, as it occurs with paper, the cotton cloth needed to be patterned to achieve that the sample and reagent flow through a specific

path. For this reason, the designed pattern (Fig. 2) comprises of several parts: *(i)* a sampling zone were the sweat is recollected or added, *(ii)* a sensing area were the **AD-VS-1** is immobilized, and *(iii)* a passive pump path in which the sample flows to reach *(iv)* an absorbent U-shaped material that makes it possible the use for a prolonged operation.

Before the optimization of the µCAD preparation, the analytical parameter used to characterize the color change of the immobilized **AD-VS-1** was selected. For this purpose, several small cotton pieces were prepared as described in Section S9 and tested on pH solutions ranged from 4 to 9 (n=3), recording and analysing the color in the RGB and HSV color spaces (See Fig. S13). The Hue (H) parameter showed a higher color variation at lower pH with lower error bars reason by that was used for the study (See Fig. S14).

Once H was selected as analytical parameter and the µCAD was designed and fabricated, different parameters related to the immobilization of the **AD-VS-1** were studied. Firstly, the volume that must be added to the sensing area was evaluated in order to cover the circle in a reproducible way. For this purpose, different volumes ranging from 0.1 to 0.5 µL of a Brilliant Blue solution (10 $mg \cdot mL^{-1}$) were added, being 0.3 µL the volume that best and most homogeneously covered the sensing area (See Fig. S15). Later, and based on the obtained results, the same test was performed using a 10 $mg \cdot mL^{-1}$ **AD-VS-1** in DMSO solution to confirm these results. In this case, the volume that best covered the sensing area was 0.2 µL. The volume needed in this case was lower due to the used solvent, since Brilliant Blue solution was solved in water, while **AD-VS** was in DMSO and it affected to the wicking on cloth.

Later, the concentration of **AD-VS-1** solution in DMSO was optimized. For this purpose, different **AD-VS-1** solutions from 1.5 to 20 $mg \cdot mL^{-1}$ (see Section S8) were tested, resulting that 15 $mg \cdot mL^{-1}$ was the concentration that best results provided in terms of CV as well as pH range of variation of the signal, being the one whose H value changed at lower pH (see Section S7).

Finally, two different procedures to prepare the µCAD were assayed. In the first procedure, the cloth was first patterned and later the reagent was immobilized. In the second procedure, these steps were followed in reverse order. The obtained results (see Fig. S17) proved that the procedure providing best results in terms of reproducibility was the patterning followed by the immobilization of the **AD-VS-1**.

2.2. Readout and processing electronics

The readout module comprises as main electronic components a low-power microcontroller unit (MCU) model PIC12LF1822 (Microchip Technology Inc., Chandler, Arizona, USA); a Bluetooth module Bluefruit Low Energy (BLE) UART Friend (Adafruit, New York, USA); a high-resolution digital color detector model S11059-02DT (Hamamatsu Photonics, Japan); a white excitation LED; and a rechargeable battery of 3.7 V and 150 mA·h capacity model JJR/C H36-004 (Goolsky, Singapore, Asia). Fig. 2(d) shows the block diagram of the processing electronics.

The sensing module, which comprises of the excitation LED and the color detector, is placed aligned in front of the pH-sensitive membrane, as shown in Fig. 2(e). The selected color detector S11059-02DT is sensitive to red (λ_{peak}=615 nm), green (λ_{peak} =530 nm), blue (λ_{peak} =460 nm), and near infrared (λ_{peak} =855 nm) incident radiation, codifying it in four 16-bit digital words. These words are sent to the MCU by means of an I^2C interface for further processing. The excitation LED is synchronised with the reading protocol of the color detector. The selected LED is white since the parameter to be determined is the color of the sensitive membrane. After the processing, the MCU sends the data to the Bluetooth module via Universal Asynchronous Receiver-Transmitter (UART) protocol. The processed data is then wirelessly transmitted to a mobile phone via Bluetooth. Fig. 2(f) shows the 3D views and real image of the fabricated readout module.

A 3D-printed plastic case was designed and fabricated (see Fig. S9) to ensure the correct alignment and positioning of the pH sensor with respect to the LED and color detector, while providing a uniform dark environment for the color measurements. In addition, to transmit the data in real-time from the wristband to the user, a custom-designed Android™ application was developed. More detailed description and screen captures of the application can be found in Section 6 of ESI.

3. Results and Discussion

3.1. Selection, synthesis and characterization of the acidochromic dye indicator AD-VS-1

Parallel advances in chemical sensing and wireless communication technologies have sparked the development of wireless chemical sensors. In this work, our engineering design is based on the use of µCAD as an optical sensor for the detection and determination of pH as the analyte. In this respect, acidochromism evolved for the sensing area of the µCAD by means of an immobilized acidochromic indicator dye as a recognition element was thought to be an adequate methodology (Mohr et al., 2008). Among the different suitable dyes, our selection was based in the appealing features of vinyl sulfone azo dyes (**AD-VS**). These compounds combine the outstanding optical properties of azo chromophores with the relatively high reactivity of the vinyl sulfone group (VS) (López-Jaramillo et al., 2012; Morales-Sanfrutos et al., 2010). The reactivity of the VS functional group fulfils most of the essential requirements needed for covalent immobilization of the azo dye to cotton cloth as the support of choice for the µCAD fabrication: *(i)* a complementary reactivity with the intrinsic nucleophilic OH present in cellulose that react by a Michael-type addition, *(ii)* a high stability of the resulting ether link, *(iii)* it takes place in an aqueous milieu, and *(iv)* a simplified one-step procedure that minimize the operational. On the base of these outstanding features **AD-VS** have found application in textile chemistry (Mohr, 2018) and they also have demonstrated their value in the fabrication of devices for optical pH-sensing (Chauhan et al., 2014; Kassal et al., 2017; Mohr et al., 2008; Werner and Wolfbeis, 1993).

Considering the current state-of-the-art, we decided to prepare a novel member of this family of compounds, named **AD-VS-1** (Fig. 2(a)), as suitable for our purposes. We envisaged an easy strategy based in a straightforward two-step procedure that starts from 4-aminothiophenol (See Supporting Information). After treatment of this aromatic compound with divinyl sulfone, that led exclusively to the corresponding thia-Michael reaction addition intermediate due to the higher nucleophility of the sulfur atom respecting to the amino group, concomitant diazotation reaction with 2,6-dimethoxyphenol afforded the desired **AD-VS-1.** Spectroscopic characterization of this indicator dye confirms this molecular structure which optical profile (absorbance spectra and molar extinction coefficient in DMSO solution) was also determined.

3.2. µCAD and pH sensor performance

As can be observed in Fig. 2(b-c), the hydrophilic section of the µCAD is composed by a sensing area and two paths: the sampling path (2.5 mm x 11.0 mm) and the passive pump path (2.5 mm x 8.1 mm). A 2.5-mm wide path was selected since it was the narrowest path that could be screen-printed on the cloth in the reproducible way. The length of both paths, sensing area size, and position in the 22.8 mm x 32.4 mm piece of cloth used to fabricate the µCAD, were selected based on the PCB and 3D-printed plastic case design.

After the µCAD design and optimization, a calibration was conducted by dipping the µCAD in 10 different standard solutions with pH from 4 to 10 during 30 s in each solution. Six different µCAD were used for the calibration. In three of them, the calibration was conducted by rising the pH value of the standard solution, while in the other three cases the pH was diminished during the calibration. This strategy was chosen to prove that the obtained H value was independent from the pH variation direction. As it can be observed in Fig. S18 the obtained results were independent from the rising or diminishing of the pH value, so the six replicates were used to obtain a Boltzmann equation fitting the data set (R^2=0.997) (see Fig. S19).

The results of this first study indicate that the designed µCAD can be used to determine the pH of sweat with good precision and within the range of the sample. However, at this stage it cannot be claimed yet that the µCAD could be used for real-time determination of pH sweat. The reason behind this is that the µCAD hydrophilic area is so small that it will be full of sample in a very short period of time. Because of that, some material needed to be included for the purpose of continuously retiring sample from the hydrophilic area of the µCAD to allow that new sample could continue flowing through it. This would ensure that the µCAD could be used during longer periods of time before saturating. The strategy followed was the inclusion of a passive pump in the µCAD, along with an absorbent pad containing Flexicel (P&G Spain, Madrid) skirting the hydrophilic area (see Fig. 2(b-c)). Flexicel is a superabsorbent material that can absorb around 20 times its weight (see the slope of the calibration function in Fig. S20(a)). This material has been successfully used as passive pump in other microfluidic devices that can be found in the literature (Suarez et al., 2020). The area of the absorbent pad used in our

design was 689 mm^2. Based on the calibration of the material and considering a sweat rate of 0.01 $\mu L \cdot s^{-1}$ (in around 15 mm^2 area) (Godek et al., 2008), the µCAD along with the absorbent pad could be used continuously up to 1058 min. Size and shape of the absorbent material was selected based in the 3D-printed plastic case, to be easy-to-place inside while maintaining its position inside along the use of the device.

A new calibration was conducted, on this occasion with the µCAD including the passive pump. In this case, a syringe pump was used to apply the sample on the sampling zone (see Fig. 2(b)) at a flow rate similar to the human sweat rate (0.01 $\mu L \cdot s^{-1}$). Each pH standard solution was applied to the µCAD during two minutes and videotaped. From the obtained results (see Fig. S21) it can be observed that only 90 seconds were enough to get a steady signal, which was used to obtain the calibration function (see Fig. 3) The data fits as previously described to a Boltzmann equation (R^2=0.996) (Eq. S2), and the range of use of the µCAD is from 6.1 to 8.4 (pKa=7.4), range in which the pH of sweat is included. The precision tested at different pH goes from 2.3 to 3.6 % (see Table 1).

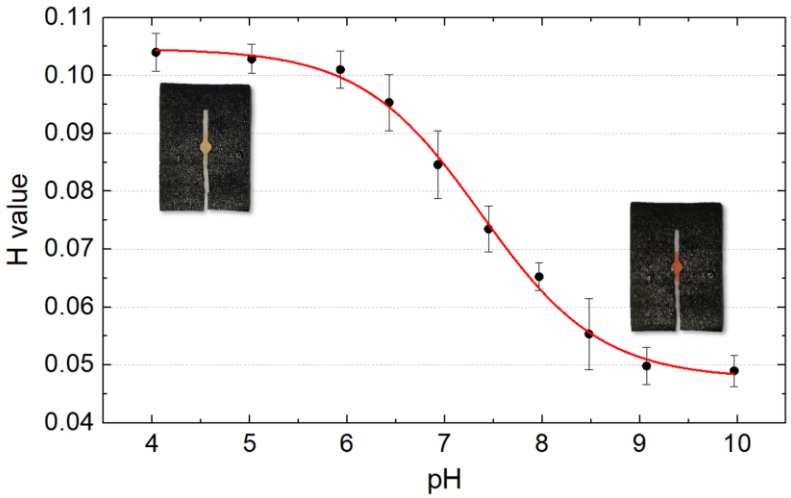

Fig. 3. Calibration of the µCAD adding the standards solution using a syringe pump at a rate of 0.01 $\mu L \cdot s^{-1}$.

Table 1. Analytical parameters of µCAD.

Analytical parameters			
A_1	0.104	**Precision (n=10)**	
A_2	0.047	**pH**	**CV (%)**
A_3	7.372		
A_4	0.614	4.04	2.5
R^2	0.996	7.45	3.5
LOD	6.1	7.97	2.3
Range	6.1 - 8.4	9.97	3.6

Due to the nature of the sweat sample, whose pH can rise or diminish indistinctly during an exercise session, an additional study was conducted to prove that the µCAD is fully reversible to pH variations. Fig. S22 shows that the µCADs are fully reversible after subjecting them to a cycle of acidic-basic-acidic pH and basic-acidic-basic pH, respectively. Finally, a stability study was performed by studying the H value of three different µCADs along 20 weeks. This study showed that, once prepared, the µCAD can be stored for 7 weeks (Fig. S23). Once the µCAD was fully characterized, seven different samples were analysed using the µCAD and the obtained results were compared to the ones provided by a pH-meter (Section S16).

3.3. Wristband performance and evaluation

As indicated in the previous section, the µCAD was analytically characterized for pH sensing and a calibration function was obtained using a camera to register the color variations (see Fig. 3). At this stage, the whole system was characterized using the optimized µCAD in combination with the readout and processing electronics. Thus, the way of registering the color changes in the µCAD due to the sweat pH was conducted through the digital color sensor included in the readout circuit (see Fig. 4(a-b)). For the calibration, a similar setup than the previous case was employed, i.e. a syringe pump was used to apply the sample on the sampling zone at a flow rate similar to the human sweat rate (0.01 $\mu L \cdot s^{-1}$). Each pH standard solution was applied to the µCAD during two minutes and the color measurements from the digital sensor were transmitted every second to the smartphone app via Bluetooth. Fig. 4(c) shows the obtained calibration curve, that can be again fitted to a Boltzmann curve (R^2=0.997) (Eq. S2). In this case, the range of use of the µCAD ranges from 6.0 to 8.0, and the precision at different pH values goes from 3.6 to 6.0 % (see Table 2). In addition, the system was tested in real-life conditions by wearing it on the wrist while exercising and transmitting the data in real-time to a smartphone via Bluetooth. Fig. 4(d) shows the experimental setup and the obtained results. It can be observed that during the first 10 min of physical activity the low sweat rate is not enough to wet the cloth sensor. After that, the pH increases due to the decrease of lactic acid in sweat.

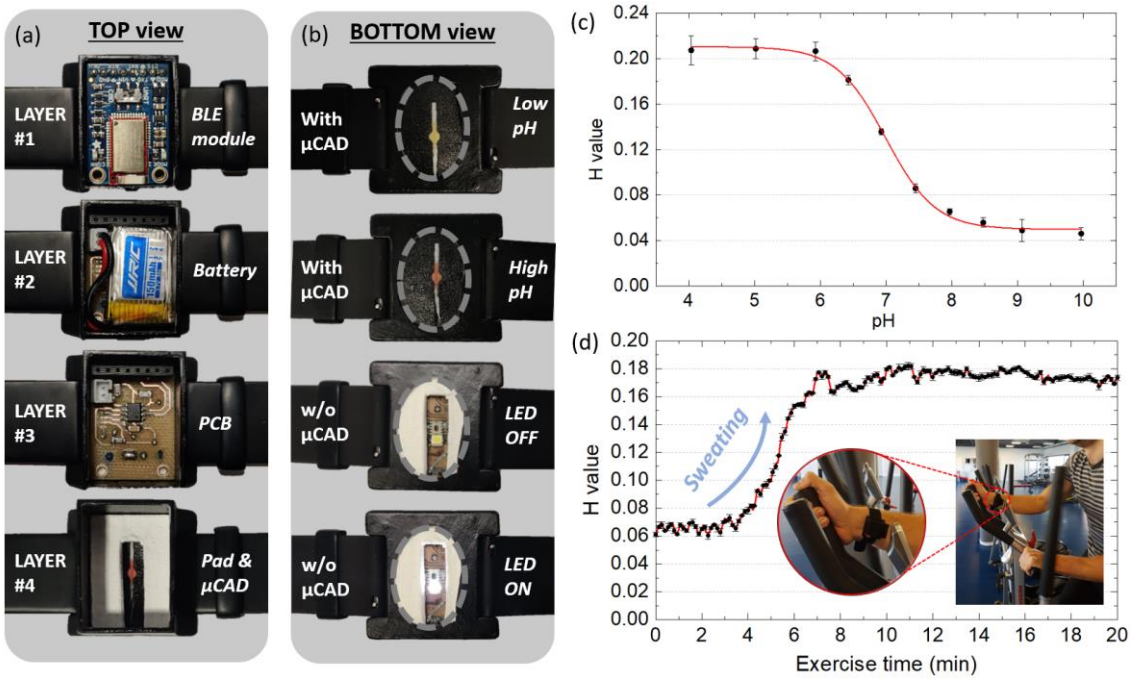

Fig. 4. (a) Layer by layer top view of the wristband, including: *1)* Low-Energy Bluetooth module, *2)* battery, *3)* PCB, and *4)* absorbent pad with µCAD; (b) Bottom view of the wristband (uncovered) with and without the µCAD layer to allow the view of the LED and color detector; (c) Calibration curve of the wristband wearable system in terms of H value; (d) Real-time results of the wearable system placed on the wristband during exercise.

Table 2. Analytical parameters of the wristband.

Analytical parameters			
$\mathbf{A_1}$	0.210	**Precision (n=10)**	
$\mathbf{A_2}$	0.050	**pH**	**CV (%)**
$\mathbf{A_3}$	0.699	6.00	4.0
$\mathbf{A_4}$	0.377	6.43	6.0
$\mathbf{R^2}$	0.997	6.93	4.5
LOD	6.0	7.45	4.3
Range	6.0 - 8.0	7.97	3.6

Overall, the developed system is convenient in terms of portability, ease of use and wearability. A number of previous works have focused on the development of sensing patches for sweat pH monitoring (Curto et al., 2012; He et al., 2019; A. Koh et al., 2016; Morris et al., 2009; Zhao et al., 2020), but they lacked the associated readout and processing electronics to obtain and transmit in real-time the measured information to the end user. In contrast to the RFID/NFC-based platforms for pH sweat sensing than can be found in previous literature (Bandodkar et al., 2019; Boada et al., 2019; Xu et al., 2019), our proposed wristband does not require that the external reader is permanently placed in its close proximity, thus allowing a truly continuous real-time monitoring. In return, our system requires a battery for its operation, which is not needed in the case of RFID/NFC

devices with energy harvesting capabilities (Dang et al., 2018). However, the use of low-power components in combination with the non-continuous measurement strategy allows a long battery life of more than 2 days (see Section S14). In terms of response speed, our system only takes 90 seconds to get a steady signal in the sensing zone through the use of the passive pump to collect the sweat, which is significantly lower than the time required in other systems to get the first readings (Liu et al., 2016). Besides, the proposed wristband is distinguished from previous sweat pH monitoring systems in two more aspects: firstly, it features a very compact design with a size similar to a wristwatch, making it more comfortable to use than other devices that must be placed, for instance, in the back; and secondly, it is completed by a custom-developed user-friendly smartphone application (Alizadeh et al., 2018; Anastasova et al., 2017; Morris et al., 2009; Nyein et al., 2018).

4. Conclusions

A wearable wristband for sweat pH wireless monitoring was developed combining a custom-designed μCAD and associated readout and processing electronics. The μCAD was designed in 100% cotton cloth by immobilizing an acidochromic dye (**AD-VS-1**). The μCAD consists of a sampling area to collect the sweat, a colorimetric sensing area, a passive pump path, and an absorbent pad that allows continuous operation up to 100 min if we consider a typical human sweat rate (0.01 $\mu L \cdot s^{-1}$). The H value in the HSV color space was selected as the best parameter to correlate the color change in the sensing area due to the pH variations. The readout module consists of a low-power microcontroller unit that controls a white LED and a digital color sensor to detect the color variations in the μCAD sensing area. In addition, a Bluetooth module transmits in real-time the measurements to a friendly-user smartphone application. The analytical characterization of the μCAD alone showed that the H parameter can be related to the sweat pH value and fitted to a Boltzmann equation (R^2=0.996). The range of use of the μCAD goes from 6.1 to 8.4, which includes the pH range of sweat. The precision tested at different pH values goes from 2.3 to 3.6 %. When compared to a commercial pH-meter with different samples, the error in the determination was around 2% in almost all the cases. The analytical characterization of the wristband as a whole showed a good fitting (R^2=0.997 in the Boltzmann equation) with a range of use from 6 to 8 and a precision at different pH values from 3.6 to 6.0 %. With an estimated battery life up to 2.63 days in non-continuous sensing mode, the developed system has potential applications in the field of personal health assessment.

Declaration of interests

The authors declare that they have no known competing financial interests or personal relationships that could have appeared to influence the work reported in this paper.

Acknowledgements

This work was founded by Spanish "Ministerio de Economía y Competitividad" (Projects PID2019-103938RB-I00 and CTQ2017-86125-P) and Junta de Andalucía (Projects B-

FQM-243-UGR18 and P18-RT-2961). The projects were partially supported by European Regional Development Funds (ERDF).

References

Alizadeh, A., Burns, A., Lenigk, R., Gettings, R., Ashe, J., Porter, A., McCaul, M., Barrett, R., Diamond, D., White, P., Skeath, P., Tomczak, M., 2018. A wearable patch for continuous monitoring of sweat electrolytes during exertion. Lab Chip 18, 2632–2641. https://doi.org/10.1039/c8lc00510a

An, B.W., Shin, J.H., Kim, S.-Y., Kim, J., Ji, S., Park, J., Lee, Y., Jang, J., Park, Y.-G., Cho, E., Jo, S., Park, J.-U., 2017. Smart Sensor Systems for Wearable Electronic Devices. Polymers (Basel). 9, 303. https://doi.org/10.3390/polym9080303

Anastasova, S., Crewther, B., Bembnowicz, P., Curto, V., Ip, H.M., Rosa, B., Yang, G.Z., 2017. A wearable multisensing patch for continuous sweat monitoring. Biosens. Bioelectron. 93, 139–145. https://doi.org/10.1016/j.bios.2016.09.038

Anastasova, S., Crewther, B., Bembnowicz, P., Curto, V., Ip, H.M., Rosa, B., Zhong-Yang, G., 2016. A Wearable Multisensing Patch for Continuous Sweat Monitoring. Biosens. Bioelectron. https://doi.org/10.1016/j.bios.2016.09.038

Bandodkar, A.J., Gutruf, P., Choi, J., Lee, K., Sekine, Y., Reeder, J.T., Jeang, W.J., Aranyosi, A.J., Lee, S.P., Model, J.B., Ghaffari, R., Su, C.-J., Leshock, J.P., Ray, T., Verrillo, A., Thomas, K., Krishnamurthi, V., Han, S., Kim, J., Krishnan, S., Hang, T., Rogers, J.A., 2019. Battery-free, skin-interfaced microfluidic/electronic systems for simultaneous electrochemical, colorimetric, and volumetric analysis of sweat. Sci. Adv. 5, eaav3294. https://doi.org/10.1126/sciadv.aav3294

Boada, M., Lazaro, A., Villarino, R., Girbau, D., 2019. Battery-Less NFC Sensor for pH Monitoring. IEEE Access 7, 33226–33239. https://doi.org/10.1109/ACCESS.2019.2904109

Boutry, C.M., Beker, L., Kaizawa, Y., Vassos, C., Tran, H., Hinckley, A.C., Pfattner, R., Niu, S., Li, J., Claverie, J., Wang, Z., Chang, J., Fox, P.M., Bao, Z., 2019. Biodegradable and flexible arterial-pulse sensor for the wireless monitoring of blood flow. Nat. Biomed. Eng. 3, 47–57. https://doi.org/10.1038/s41551-018-0336-5

Chacon, P.J., Pu, L., da Costa, T.H., Shin, Y.H., Ghomian, T., Shamkhalichenar, H., Wu, H.C., Irving, B.A., Choi, J.W., 2018. A Wearable Pulse Oximeter with Wireless Communication and Motion Artifact Tailoring for Continuous Use. IEEE Trans. Biomed. Eng. 66, 1505–1513. https://doi.org/10.1109/TBME.2018.2874885

Chauhan, P., Hadad, C., López, A.H., Silvestrini, S., La Parola, V., Frison, E., Maggini, M., Prato, M., Carofiglio, T., 2014. A nanocellulose–dye conjugate for multi-format optical pH-sensing. Chem. Commun. 50, 9493–9496. https://doi.org/10.1039/C4CC02983F

Choi, J., Ghaffari, R., Baker, L.B., Rogers, J.A., 2018. Skin-interfaced systems for sweat collection and analytics. Sci. Adv. 4, 1–10. https://doi.org/10.1126/sciadv.aar3921

Chung, M., Fortunato, G., Radacsi, N., 2019. Wearable flexible sweat sensors for healthcare monitoring: A review. J. R. Soc. Interface 16. https://doi.org/10.1098/rsif.2019.0217

Curto, V.F., Fay, C., Coyle, S., Byrne, R., O'Toole, C., Barry, C., Hughes, S., Moyna, N., Diamond, D., Benito-Lopez, F., 2012. Real-time sweat pH monitoring based on a wearable chemical barcode micro-fluidic platform incorporating ionic liquids. Sensors Actuators B Chem. 171–172, 1327–1334. https://doi.org/10.1016/j.snb.2012.06.048

Dang, W., Manjakkal, L., Navaraj, W.T., Lorenzelli, L., Vinciguerra, V., Dahiya, R., 2018. Stretchable wireless system for sweat pH monitoring. Biosens. Bioelectron. 107, 192–202. https://doi.org/10.1016/j.bios.2018.02.025

Gao, W., Emaminejad, S., Nyein, H.Y.Y., Challa, S., Chen, K., Peck, A., Fahad, H.M., Ota, H., Shiraki, H., Kiriya, D., Lien, D.-H., Brooks, G.A., Davis, R.W., Javey, A., 2016. Fully integrated wearable sensor arrays for multiplexed in situ perspiration analysis. Nature 529, 509–514. https://doi.org/10.1038/nature16521

Gao, W., Ota, H., Kiriya, D., Takei, K., Javey, A., 2019. Flexible Electronics toward Wearable

Sensing. Acc. Chem. Res. 52, 523–533. https://doi.org/10.1021/acs.accounts.8b00500
Godek, S.F., Bartolozzi, A.R., Burkholder, R., Sugarman, E., Peduzzi, C., 2008. Sweat Rates and Fluid Turnover in Professional Football Players: A Comparison of National Football League Linemen and Backs. J. Athl. Train. 43, 184–189. https://doi.org/10.4085/1062-6050-43.2.184
Güder, F., Ainla, A., Redston, J., Mosadegh, B., Glavan, A., Martin, T.J., Whitesides, G.M., 2016. Paper-Based Electrical Respiration Sensor. Angew. Chemie Int. Ed. 55, 5727–5732. https://doi.org/10.1002/anie.201511805
He, X., Xu, T., Gu, Z., Gao, W., Xu, L.-P., Pan, T., Zhang, X., 2019. Flexible and Superwettable Bands as a Platform toward Sweat Sampling and Sensing. Anal. Chem. 91, 4296–4300. https://doi.org/10.1021/acs.analchem.8b05875
Heikenfeld, J., Jajack, A., Feldman, B., Granger, S.W., Gaitonde, S., Begtrup, G., Katchman, B.A., 2019. Accessing analytes in biofluids for peripheral biochemical monitoring. Nat. Biotechnol. 37, 407–419. https://doi.org/10.1038/s41587-019-0040-3
Jeong, I.C., Bychkov, D., Searson, P.C., 2019. Wearable devices for precision medicine and health state monitoring. IEEE Trans. Biomed. Eng. 66, 1242–1258. https://doi.org/10.1109/TBME.2018.2871638
Kansara, R., Bhojani, P., Chauhan, J., 2018. Designing Smart Wearable to measure Health Parameters, in: 2018 International Conference on Smart City and Emerging Technology (ICSCET). IEEE, pp. 1–5. https://doi.org/10.1109/ICSCET.2018.8537314
Kassal, P., Zubak, M., Scheipl, G., Mohr, G.J., Steinberg, M.D., Murković Steinberg, I., 2017. Smart bandage with wireless connectivity for optical monitoring of pH. Sensors Actuators B Chem. 246, 455–460. https://doi.org/10.1016/j.snb.2017.02.095
Kaya, T., Liu, G., Ho, J., Yelamarthi, K., Miller, K., Edwards, J., Stannard, A., 2019. Wearable Sweat Sensors: Background and Current Trends. Electroanalysis 31, 411–421. https://doi.org/10.1002/elan.201800677
Kim, J., Sempionatto, J.R., Imani, S., Hartel, M.C., Barfidokht, A., Tang, G., Campbell, A.S., Mercier, P.P., Wang, J., 2018. Simultaneous Monitoring of Sweat and Interstitial Fluid Using a Single Wearable Biosensor Platform. Adv. Sci. 5. https://doi.org/10.1002/advs.201800880
Koh, Ahyeon, Kang, D., Xue, Y., Lee, S., Pielak, R.M., Kim, J., Hwang, T., Min, S., Banks, A., Bastien, P., Manco, M.C., Wang, L., Ammann, K.R., Jang, K.-I., Won, P., Han, S., Ghaffari, R., Paik, U., Slepian, M.J., Balooch, G., Huang, Y., Rogers, J.A., 2016. A soft, wearable microfluidic device for the capture, storage, and colorimetric sensing of sweat. Sci. Transl. Med. 8, 366ra165-366ra165. https://doi.org/10.1126/scitranslmed.aaf2593
Koh, A., Kang, D., Xue, Y., Lee, S., Pielak, R.M., Kim, J., Hwang, T., Min, S., Banks, A., Bastien, P., Manco, M.C., Wang, L., Ammann, K.R., Jang, K.-I., Won, P., Han, S., Ghaffari, R., Paik, U., Slepian, M.J., Balooch, G., Huang, Y., Rogers, J.A., 2016. A soft, wearable microfluidic device for the capture, storage, and colorimetric sensing of sweat. Sci. Transl. Med. 8, 366ra165-366ra165. https://doi.org/10.1126/scitranslmed.aaf2593
Liu, G., Ho, C., Slappey, N., Zhou, Z., Snelgrove, S.E., Brown, M., Grabinski, A., Guo, X., Chen, Y., Miller, K., Edwards, J., Kaya, T., 2016. A wearable conductivity sensor for wireless real-time sweat monitoring. Sensors Actuators B Chem. 227, 35–42. https://doi.org/10.1016/j.snb.2015.12.034
López-Jaramillo, F.J., Hernández-Mateo, F., Santoyo-González, F., 2012. Vinyl Sulfone: A Multi-Purpose Function in Proteomics, in: Integrative Proteomics. InTech. https://doi.org/10.5772/29682
Lopez-Ruiz, N., Curto, V.F., Erenas, M.M., Benito-Lopez, F., Diamond, D., Palma, A.J., Capitan-Vallvey, L.F., 2014. Smartphone-Based Simultaneous pH and Nitrite Colorimetric Determination for Paper Microfluidic Devices. Anal. Chem. 86, 9554–9562. https://doi.org/10.1021/ac5019205
Lu, Y., Jiang, K., Chen, D., Shen, G., 2019. Wearable sweat monitoring system with integrated micro-supercapacitors. Nano Energy 58, 624–632. https://doi.org/10.1016/j.nanoen.2019.01.084
Manas, M., Sinha, A., Sharma, S., Mahboob, M.R., 2018. A novel approach for IoT based

545 wearable health monitoring and messaging system. J. Ambient Intell. Humaniz. Comput.
546 10, 2817–2828. https://doi.org/10.1007/s12652-018-1101-z
547 MarketsandMarkets, 2016. Wearable Fitness Technology Market [WWW Document]. URL
548 https://www.marketsandmarkets.com/Market-Reports/wearable-fitness-technology-
549 market-139869705.html
550 Martín, A., Kim, J., Kurniawan, J.F., Sempionatto, J.R., Moreto, J.R., Tang, G., Campbell, A.S.,
551 Shin, A., Lee, M.Y., Liu, X., Wang, J., 2017. Epidermal Microfluidic Electrochemical
552 Detection System: Enhanced Sweat Sampling and Metabolite Detection. ACS Sensors 2,
553 1860–1868. https://doi.org/10.1021/acssensors.7b00729
554 Mohr, G.J., 2018. Synthesis of naphthalimide-based indicator dyes with a 2-
555 hydroxyethylsulfonyl function for covalent immobilisation to cellulose. Sensors Actuators
556 B Chem. 275, 439–445. https://doi.org/10.1016/j.snb.2018.07.095
557 Mohr, G.J., Müller, H., Bussemer, B., Stark, A., Carofiglio, T., Trupp, S., Heuermann, R.,
558 Henkel, T., Escudero, D., González, L., 2008. Design of acidochromic dyes for facile
559 preparation of pH sensor layers. Anal. Bioanal. Chem. 392, 1411–1418.
560 https://doi.org/10.1007/s00216-008-2428-7
561 Morales-Sanfrutos, J., Lopez-Jaramillo, J., Ortega-Muñoz, M., Megia-Fernandez, A., Perez-
562 Balderas, F., Hernandez-Mateo, F., Santoyo-Gonzalez, F., 2010. Vinyl sulfone: a versatile
563 function for simple bioconjugation and immobilization. Org. Biomol. Chem. 8, 667–675.
564 https://doi.org/10.1039/B920576D
565 Morris, D., Coyle, S., Wu, Y., Lau, K.T., Wallace, G., Diamond, D., 2009. Bio-sensing textile
566 based patch with integrated optical detection system for sweat monitoring. Sensors
567 Actuators B Chem. 139, 231–236. https://doi.org/10.1016/j.snb.2009.02.032
568 Nikolajek, W.P., Emrich, H.M., 1976. pH of sweat of patients with cystic fibrosis. Klin.
569 Wochenschr. 54, 287–288. https://doi.org/10.1007/BF01468925
570 Noakes, T.D., 1992. The hyponatremia of exercise. Int. J. Sport Nutr. 2, 205–228.
571 Nyein, H.Y.Y., Tai, L., Ngo, Q.P., Chao, M., Zhang, G.B., Gao, W., Bariya, M., Bullock, J.,
572 Kim, H., Fahad, H.M., Javey, A., 2018. A Wearable Microfluidic Sensing Patch for
573 Dynamic Sweat Secretion Analysis. ACS Sensors 3, 944–952.
574 https://doi.org/10.1021/acssensors.7b00961
575 Olanrewaju, A., Beaugrand, M., Yafia, M., Juncker, D., 2018. Capillary microfluidics in
576 microchannels: from microfluidic networks to capillaric circuits. Lab Chip 18, 2323–2347.
577 https://doi.org/10.1039/C8LC00458G
578 Ortega, L., Llorella, A., Esquivel, J.P., Sabaté, N., 2019. Self-powered smart patch for sweat
579 conductivity monitoring. Microsystems Nanoeng. 5, 3. https://doi.org/10.1038/s41378-
580 018-0043-0
581 Parrilla, M., Guinovart, T., Ferré, J., Blondeau, P., Andrade, F.J., 2019. A Wearable Paper-
582 Based Sweat Sensor for Human Perspiration Monitoring. Adv. Healthc. Mater. 8,
583 1900342. https://doi.org/10.1002/adhm.201900342
584 Patterson, M.J., Galloway, S.D.R., Nimmo, M.A., 2002. Effect of induced metabolic alkalosis
585 on sweat composition in men. Acta Physiol. Scand. 174, 41–46.
586 https://doi.org/10.1046/j.1365-201x.2002.00927.x
587 Perry, T.S., 2018. Wearable sensor detects stress in sweat. IEEE Spectr. 55, 14–15.
588 https://doi.org/10.1109/MSPEC.2018.8449037
589 Riaz, F., Azad, M.A., Arshad, J., Imran, M., Hassan, A., Rehman, S., 2019. Pervasive blood
590 pressure monitoring using Photoplethysmogram (PPG) sensor. Futur. Gener. Comput.
591 Syst. 98, 120–130. https://doi.org/10.1016/j.future.2019.02.032
592 Sawka, M.N., Coyle, E.F., 1999. Influence of Body Water and Blood Volume on
593 Thermoregulation and Exercise Performance in the Heat. Exerc. Sport Sci. Rev. 27, 167–
594 218. https://doi.org/10.1249/00003677-199900270-00008
595 Suarez, W.T., Franco, M.O.K., Capitán-Vallvey, L.F., Erenas, M.M., 2020. Chitosan-modified
596 cotton thread for the preconcentration and colorimetric trace determination of Co(II).
597 Microchem. J. 158, 105137. https://doi.org/10.1016/j.microc.2020.105137
598 Werner, T., Wolfbeis, O.S., 1993. Optical sensor for the pH 10-13 range using a new support
599 material. Fresenius. J. Anal. Chem. 346, 564–568. https://doi.org/10.1007/BF00321245

Xu, G., Cheng, C., Liu, Z., Yuan, W., Wu, X., Lu, Y., Low, S.S., Liu, J., Zhu, L., Ji, D., Li, S., Chen, Z., Wang, L., Yang, Q., Cui, Z., Liu, Q., 2019. Battery-Free and Wireless Epidermal Electrochemical System with All-Printed Stretchable Electrode Array for Multiplexed In Situ Sweat Analysis. Adv. Mater. Technol. 4, 1800658. https://doi.org/10.1002/admt.201800658

Zhao, F.J., Bonmarin, M., Chen, Z.C., Larson, M., Fay, D., Runnoe, D., Heikenfeld, J., 2020. Ultra-simple wearable local sweat volume monitoring patch based on swellable hydrogels. Lab Chip 20, 168–174. https://doi.org/10.1039/C9LC00911F